ELSEVIER

Materials Science and Engineering A319–321 (2001) 342–346

MATERIALS SCIENCE & ENGINEERING A

www.elsevier.com/locate/msea

Microprocesses of the deformation of single and polycrystalline $MoSi_2$

Ulrich Messerschmidt [a,*], Susanne Guder [a], Ludwig Junker [a], Martin Bartsch [a], Masaharu Yamaguchi [b]

[a] *Max-Planck-Institut für Mikrostrukturphysik, Weinberg 2, Halle/Saale D-06120, Germany*
[b] *Department of Materials Science and Engineering, Kyoto University, 606-8501 Kyoto, Japan*

Abstract

$MoSi_2$ single crystals in the soft ⟨201⟩ orientation and polycrystals were deformed in constant strain rate tests in compression between 300 and 1200°C for single crystals, and between 495 and 1250°C for polycrystals. Stress relaxation and temperature change tests were performed to determine the activation parameters of the deformation. In addition to conventional transmission electron microscopy in a high-voltage electron microscope, in situ straining experiments were carried out in this instrument to observe the deformation processes directly. A new model is proposed to interpret the flow stress anomaly in $MoSi_2$ single crystals. In polycrystals, the deformation is controlled by dislocation glide below about 1050°C, however, by decohesion of a grain boundary phase above this temperature.

Keywords: Molybdenum disilicide; Plastic deformation; Transmission electron microscopy; Flow stress anomaly

1. Introduction

Materials based on molybdenum disilicide are prospective candidates for structural applications at high temperatures, particularly as a matrix of composites (see, e.g. Ref. [1]). To understand the strength properties of these complex materials, the microprocesses of the deformation of the polycrystalline $MoSi_2$ matrix and even those of single crystals should be known. For both materials, the present study comprises the results of macroscopic deformation tests, of transmission electron microscopy in a high-voltage electron microscope (HVEM) and of in situ straining experiments inside the latter, which allow the direct observation of the microprocesses. The in situ experiments were performed in a special tensile stage for temperatures up to more than 1000°C [2]. Preliminary results were published in Refs [3,4].

2. Macroscopic deformation tests

$MoSi_2$ single crystals grown by the floating zone technique were deformed in compression along a soft ⟨201⟩ orientation at a strain rate of $10^{-5}\ s^{-1}$. For the polycrystals produced by reaction sintering and hot-pressing, a strain rate of $2.5 \times 10^{-7}\ s^{-1}$ was chosen since this material disintegrates at higher strain rates and high temperatures. Fig. 1a presents the temperature dependence of the upper yield points of both materials. The single crystals show three temperature ranges: a normal decrease between 300 and 500°C, presenting smooth deformation curves, an anomalous increase between 500 and 1000°C where jerky flow occurs, and a high-temperature decrease above 1000°C with smooth deformation again. Polycrystals show a continuous decrease of the flow stress but the slope of the curve suggests three ranges, too. Between 495 and 1000°C, there is a slight decrease of -1 MPa K^{-1} at an average, with a weak shoulder between about 750 and 900°C. Between 1050 and 1150°C, the flow stress decreases rapidly by -3 MPa K^{-1}. Above that temperature it decreases weakly to reach a very small value at 1250°C.

The strain rate sensitivity r of the flow stress σ was determined from the initial slope of stress relaxation (SR) curves plotted as $\ln(-\dot{\sigma})$ versus σ according to $r = \Delta\sigma/\Delta \ln \dot{\varepsilon} = \Delta\sigma/\Delta \ln(-\dot{\sigma})$. In addition, a few data are from strain rate cycling (SRC) tests. In Fig. 1b, the single crystals show a strong decrease of r with increasing temperature in the low-temperature range. There

* Corresponding author. Tel.: +49-345-5582927; fax: +49-345-5511223.
E-mail address: um@mpi-halle.mpg.de (U. Messerschmidt).

0921-5093/01/$ - see front matter
PII: S0921-5093(01)01101-7

are very small or even negative values (in the SRC tests) in the range of the anomaly, and increasing values in the high-temperature range. Negative values cannot be observed by SR experiments. In the anomaly range, the relaxation curves show an inverse curvature, i.e. r increases with decreasing $\dot{\varepsilon}$ or σ. The polycrystals exhibit almost constant values of r between 495 and 850°C and a strong increase above that range.

3. Observation of the microstructure

Fig. 2 presents micrographs of single crystal specimens deformed in the low-temperature and the anomaly range. In these ranges, most dislocations have $1/2\langle 111\rangle$ Burgers vectors and move on {110} planes. At low temperatures (Fig. 2a), they are relatively straight and oriented close to the 30, 60° and edge characters with respect to the Burgers vector direction. 60° dislocations along $\langle 111\rangle$ are dominating. Screw dislocations are almost missing.

In the anomaly range, the dislocations are straight again (Fig. 2b). In contrast to the deformation in the low-temperature range, 60° dislocations along $\langle 110\rangle$ become dominating with increasing temperature. Thus, the increase in the flow stress in the anomaly range is accompanied with a transition of the predominance of 60° dislocations from $\langle 111\rangle$ to $\langle 110\rangle$ directions, which are not identical crystallographically. The straight shape of the dislocations oriented along $\langle 110\rangle$ 60° or $\langle 331\rangle$ 90° is preserved also during their motion, as demonstrated in Fig. 3 taken during in situ deformation in an HVEM. The dislocations are created in localized sources emitting a large number of dislocations on the same plane. They move either in an unstable or a viscous way.

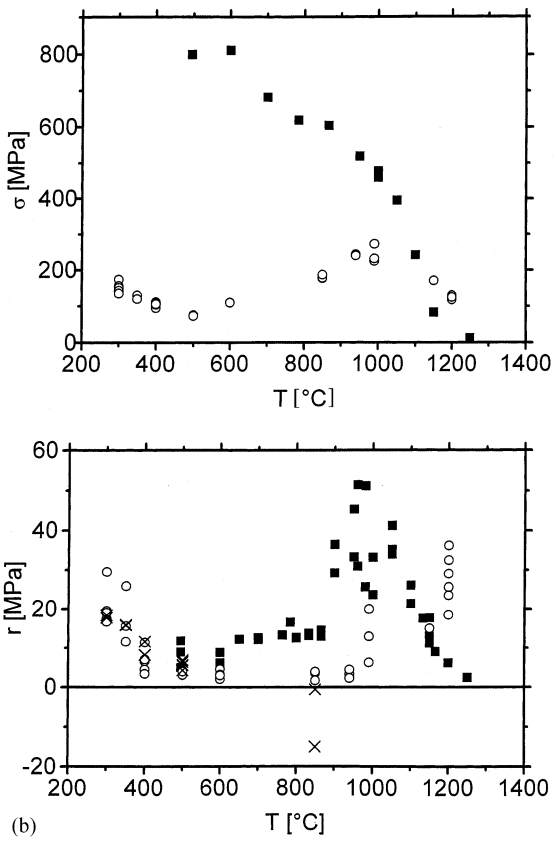

Fig. 1. Temperature dependence of deformation data of $MoSi_2$ single crystals along a $\langle 201\rangle$ orientation (open circles) and of polycrystals (solid squares). (a) (Engineering) flow stress σ at the upper yield point. (b) Strain rate sensitivity r determined from SR (squares and circles) and from SRC tests (crosses).

In the high-temperature range, the microstructure contains also single dislocations and prismatic loops with $\langle 100\rangle$ Burgers vectors. This range, in which recovery plays some role, will not be discussed here.

Below about 1050°C, polycrystals deform by slip, too. Fig. 4a and b show optical micrographs of slip steps on the specimen surface. The results of indexing the slip steps by electron back-scattered diffraction (EBSD) and of transmission electron microscopy are consistent with $\{110\}\langle 111\rangle$ and $\{011\}\langle 100\rangle$ as the most prominent slip systems. While at higher temperatures, many grains deform on two sets of intersecting slip planes, fewer grains were observed to deform at 600 and 495°C showing only a single set of slip steps. Cracks may appear at all temperatures. The density of cracks increases with the number of slip steps decreasing. Above about 1050°C, slip steps do not form. Instead, the material deforms along a grain boundary phase, with intergranular cracks appearing by grain boundary decohesion parallel to the loading direction. The viscous failure of the grain boundary phase has been proven by in situ straining experiments in the HVEM, too.

4. Discussion

The flow stresses of the $\{110\}1/2\langle 111\rangle$ slip system in single crystals following from Fig. 1a are lower than those determined previously [5]. Besides, the stress versus temperature curve is shifted to lower temperatures. Both can be due to the lower strain rate in the present study. Between 300 and 500°C, the flow stress shows its normal decrease. At 300°C, the activation volume calculated from the strain rate sensitivity data in Fig. 1b by $V = \mathrm{kT}/(m_s r)$ is about 10 b^3. Here, k is the Boltzmann constant, T, the absolute temperature, m_s, the orientation factor, and b, the absolute value of the Burgers vector. This activation volume as well as the straight shape of the dislocations, particularly the 60° dislocations in $\langle 111\rangle$ orientation are consistent with the Peierls mechanism controlling the dislocation mobility. However, an activation volume of about 100 b^3 at 500°C, i.e. at the high-temperature end of this range, points also to other glide obstacles, perhaps impurities.

The anomalous increase of the flow stress above 500°C should be initiated by an additional friction mechanism. It has been argued in [6,7] that this mechanism consists

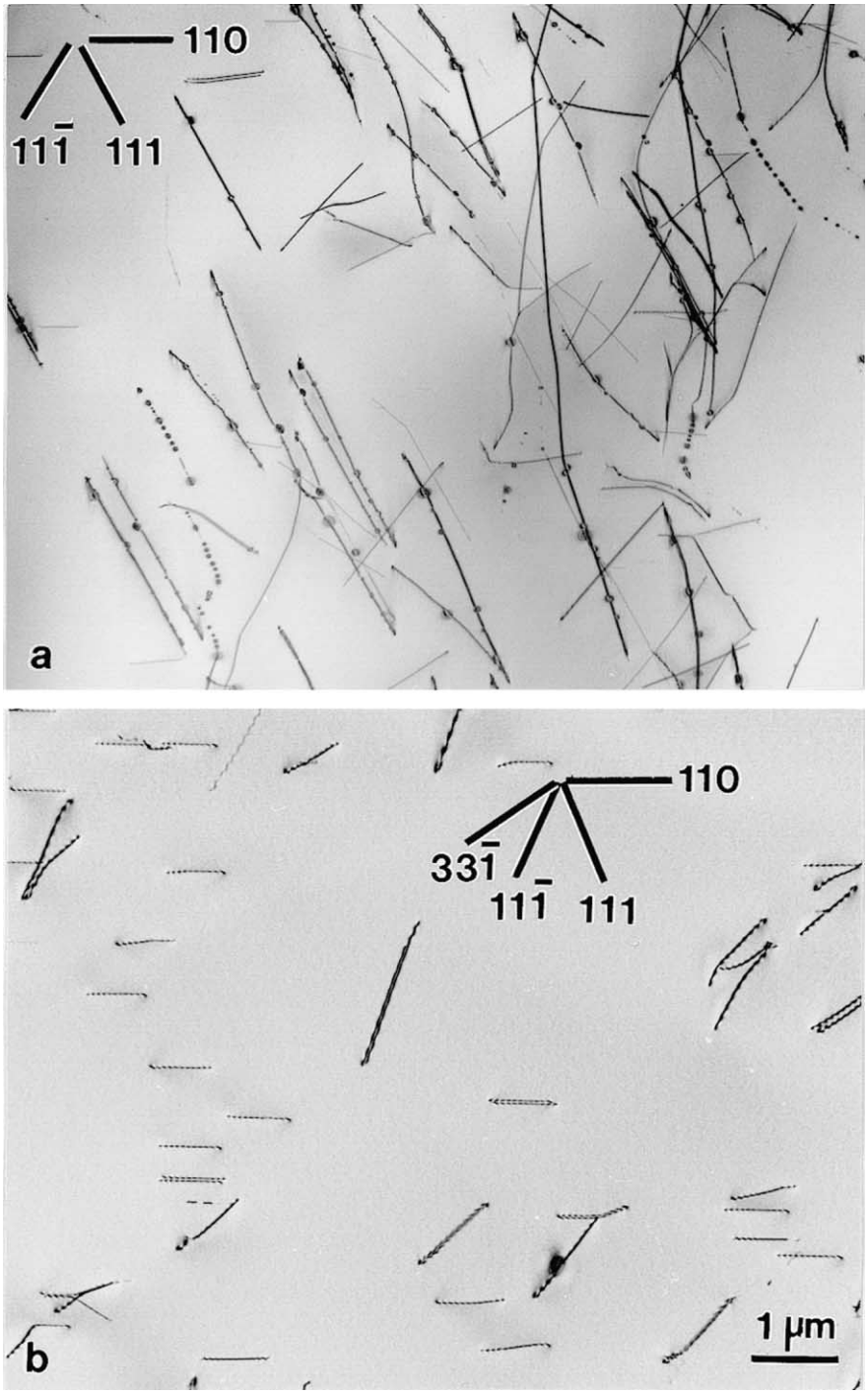

Fig. 2. Dislocation structures in $MoSi_2$ single crystals deformed along [201] taken in an HVEM. (a) 300°C, plastic strain 0.37%, beam direction (BD) $\cong [1\bar{1}0]$ perpendicular to $(1\bar{1}0)$ slip plane, Burgers vector $\mathbf{b}\|\langle 11\bar{1}\rangle$, $\mathbf{g}\|(110)$. (b) At first 500°C, then 850°C, 1.5%, BD $\cong [010]$, $\mathbf{b}\|\langle 111\rangle$, $\mathbf{g}\|(200)$. Arrows mark the projections of the indicated directions onto the image plane.

in the diffusion-controlled formation of point defect atmospheres around the dislocations. This model explains well the unstable mode of dislocation motion in macroscopic experiments, the coexistence of unstable and viscous dislocation motion, the low or even negative strain rate sensitivity of the flow stress, and the inverse curvature of the stress relaxation curves. However, unlike NiAl or TiAl, for instance, where at high temperatures the viscously moving (ordinary) dislocations are smoothly bent, the dislocations in $MoSi_2$ are straight and in crystallographic orientations. As described in Section 3 and in accordance with [5], the predominance of 60° dislocations along $\langle 111\rangle$ in the low-temperature range changes to such along $\langle 110\rangle$ within the anomaly range. Thus, the occurrence of the anomaly is certainly related to changes in the core

structure of the dislocations. Here, it is suggested that in the anomaly range, the dislocations undergo a climb dissociation according to

$$1/2[111](1\bar{1}0) \rightarrow 1/6[331](1\bar{1}0) + 1/6[3\bar{3}1](\bar{1}16) + 1/6[\bar{3}31](1\bar{1}6) \quad (1)$$

similar to the climb dissociation suggested for dislocations with $\langle 110 \rangle$ Burgers vectors in NiAl [8]. The dissociation according to Eq. (1) does not contradict the weak beam images of Fig. 1 in Ref. [9] and of Fig. 7 in Ref. [5], which resolve two partials of different contrast, but it does not agree with Fig. 10b in Ref. [10]. Calculations using anisotropic elasticity show that the dissociation according to Eq. (1) is accompanied by a 3% gain in energy. The faults between the partial dislocations are antiphase boundaries. They have high energies [11] so that the dissociation width should be small. The latter two partials cannot glide on the {110} glide plane of the total dislocation. Thus, the dissociation as well as the motion of the whole dislocation requires conservative climb in the dislocation core, which is possible solely at sufficiently high temperatures. The latter partials are pure edge components for the 60° dislocations along [110], which may explain that these dislocations experience the greatest glide resistance leading to their dominance in the dislocation structure in the anomaly range. The dynamics of the dislocation motion should be similar to that of the model of atmosphere formation explaining also the other experimental results described above. As in other materials, the dislocation mobility controlling the thermal contribution of the flow stress influences also the dislocation generation so that, finally, the flow stress in the anomaly range includes also a large athermal component.

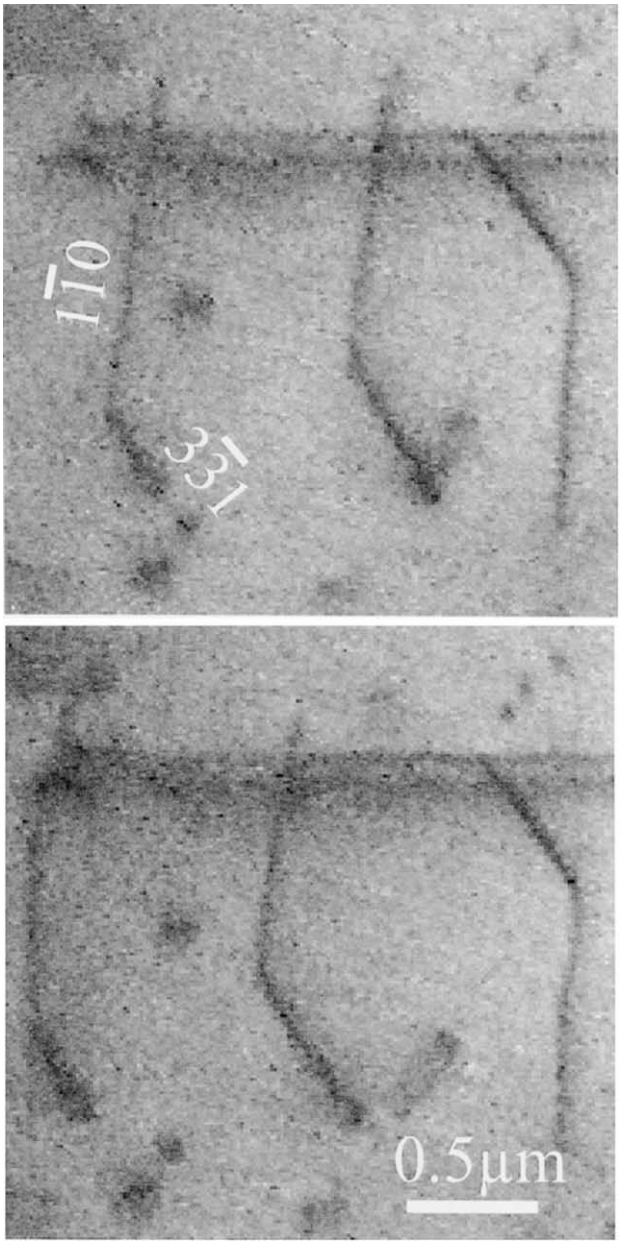

Fig. 3. Stages of a video recording of viscous motion of dislocations with $\mathbf{b} = 1/2[1\bar{1}1]$ on (110) during deformation along [201] at 1000°C inside an HVEM.

The deformation of polycrystals at about 850°C is characterized by multiple slip of easy slip systems. However, these systems do not yield the five independent slip systems necessary for continuous slip after the von Mises criterion. According to Ref. [5], several easy slip systems show a maximum of the critical resolved shear stress of about 300 MPa at about 850°C, i.e. twice the value of the $\langle 111 \rangle \{110\}$ system corresponding to Fig. 1a. Thus, considering an average orientation factor of about 0.4, the single crystal data may explain the flow stress of the polycrystals at 850°C, with the shoulder in the flow stress versus temperature curve of Fig. 1a demonstrating the flow stress anomaly. In contrast to single crystals, below 850°C, the strain rate sensitivity of polycrystals in Fig. 1b is almost independent of temperature. It corresponds to activation volumes somewhat smaller than 200 b^3. This value may be due to a larger amount of impurities in the polycrystals, mainly iron from ball milling. The impurity contribution to the flow stress will show a continuous increase at decreasing temperature but not the minimum of the single crystal data at about 500°C. In addition, the very high flow stress at low temperatures may be caused by the blocking of the narrow slip bands at the grain boundaries, finally initiating cracks. At high temperatures, $MoSi_2$ polycrystals deform by the deformation and decohesion of a grain boundary phase, which can be described by a reduction of the effective cross section and a rheological Burgers model.

The authors thank Dr W. Tirschler, Dresden, for performing the EBSD measurements, Dr D. Baither for offering his PC programme to calculate anisotropic dislocation line energies and Ch. Dietzsch and W. Greie for technical help. Financial support by the Volkswagenstiftung is gratefully acknowledged.

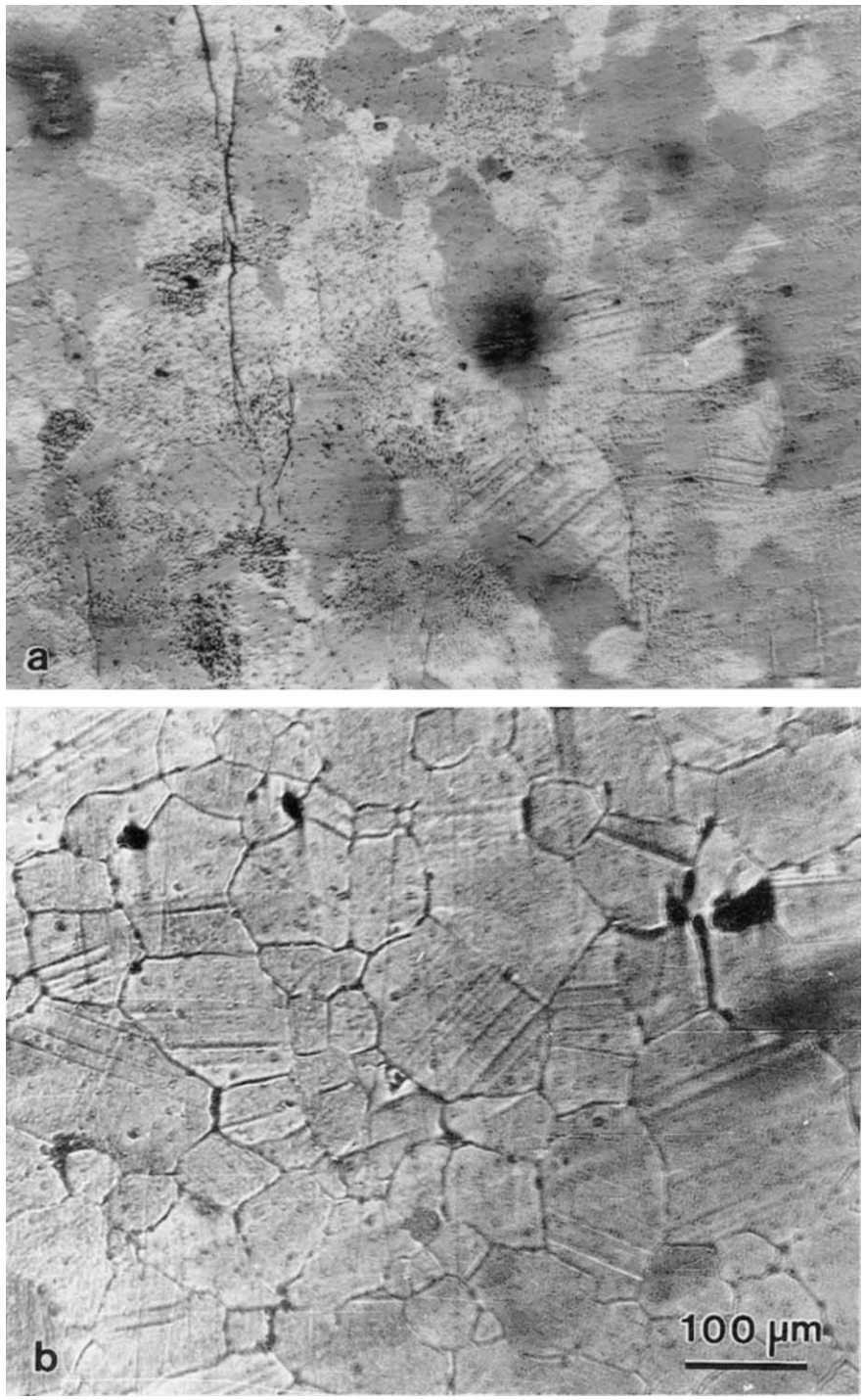

Fig. 4. Optical micrographs of deformed $MoSi_2$ polycrystals. (a) 495°C, plastic strain 0.2%; and (b) 1000°C, 0.5%.

References

[1] Proceedings of High Temperature Structural Silicides Conference, in: A.K. Vasudevan, J.J. Petrovic, S.G. Fishman, C.A. Sorrell, M.V. Nathal (Eds.), Mater. Sci. Eng. A261, 1999.
[2] U. Messerschmidt, M. Bartsch, Ultramicroscopy 56 (1994) 163.
[3] S. Guder, M. Bartsch, M. Yamaguchi, U. Messerschmidt, Mater. Sci. Eng. A261 (1999) 138.
[4] L. Junker, M. Bartsch, U. Messerschmidt, in: E.P. George, M.J. Mills, M. Yamaguchi (Eds.), High Temperature Ordered Intermetallic Alloys VIII, Materials Research Society Proceedings, Vol. 552, 1999, p. KK5.23.1.
[5] K. Ito, H. Inui, Y. Shirai, M. Yamaguchi, Philos. Mag. A72 (1995) 1075.
[6] U. Messerschmidt, M. Bartsch, S. Guder, D. Häußler, R. Haushälter, M. Yamaguchi, Intermetallics 6 (1998) 729.
[7] U. Messerschmidt, M. Bartsch, S. Guder, D. Häussler, in: E.P. George, M.J. Mills, M. Yamaguchi (Eds.), High Temperature Ordered Intermetallic Alloys VIII, Materials Research Society Proceedings, Vol. 552, 1999, p. KK10.9.1.
[8] J. Mills, R. Srinivasan, M.S. Daw, Philos. Mag. A77 (1998) 801.
[9] D.J. Evans, S.A. Court, P.M. Hazzledine, H.L. Fraser, Philos. Mag. Lett. 67 (1993) 331.
[10] S.A. Maloy, T.E. Mitchell, A.H. Heuer, Acta Metall. Mater. 43 (1995) 657.
[11] M.I. Baskes, Mater. Sci. Eng. A261 (1999) 165.